J Mater Sci (2016) 51:2869–2876
DOI 10.1007/s10853-015-9595-7

Atomistic modeling of the dissociation of a screw dislocation in silicon

L. Pizzagalli[1]

Received: 29 September 2015 / Accepted: 14 November 2015 / Published online: 24 November 2015

Abstract The nature of dislocations involved in the plastic deformation of semiconductors is different in high- and low-temperature domains. Experimental investigations have not allowed to discriminate between dissociation and nucleation as the main reason behind this transition. In this work, the mechanisms leading to the dissociation of a screw dislocation in silicon, determined by means of atomistic calculations, are described. It is shown that kink pair formation, followed by successive kink migrations, leads to the formation of two 30° partial dislocations from the screw dislocation core. These mechanisms are structurally very similar to those involved in the formation and migration of kinks in the case of a single 30° partial dislocation, because of the close resemblance between the screw and 30° dislocation cores. The calculated activation energy of the whole process is 2.14 eV, thus quite comparable to the energies involved in the propagation of partial dislocations. This shows that dissociation and nucleation processes are likely to be activated at similar temperature ranges.

Introduction

The mechanical properties of semiconductors with the cubic zinc-blende structure are relatively well known nowadays. At high temperatures, above the brittle to ductile temperature (BDT), these materials will plastically deform due to the motion of Shockley partial dislocations [1]. Below BDT instead, fracture occurs by the propagation of cracks [2]. However, this general picture is appropriate for bulk materials, since it has been recently shown to be possible to obtain a ductile behavior below the bulk BDT when one or several characteristic dimensions were reduced. Such a size effect has been demonstrated in the case of semiconductor nanowires [3–6], which are extremely important systems for nanotechnology [7, 8]. Semiconductor nano- and micro-pillars [9–13], nanospheres [14, 15], and nanobridges [16] were also the focus of extensive investigations. It is found that in these systems the BDT could be lower than in bulk materials, a phenomenon that is probably related to the growing surface influence in small dimension systems. This opens the way to the ductile deformation of semiconductors at moderate temperatures, although stresses in the GPa scale are typically required to reach plasticity [17]. Because of the continuous search to improve efficiency by reducing dimensions, such stress levels can now be obtained in real semiconductor devices [18]. For future microelectronics and nanotechnology applications, it is then essential to better understand plastic deformations occurring at low temperatures and high stresses.

Aside nanoscale systems, it is also possible to investigate this regime in macroscale samples by either scratching and indenting the surface [19–21], or using a confining pressure [22–25]. The former technique allows for reaching very high stress in a localized region, while the latter prevents the opening of crack, thus shifting fracture to higher stress levels. Available data clearly revealed that dislocations occurring at low temperature and high stress are non-dissociated [26] and are likely to be different from dislocations activated in the high-temperature regime.

An intriguing yet still unanswered question concerns the transition between the high-temperature/low-stress and

✉ L. Pizzagalli
Laurent.Pizzagalli@univ-poitiers.fr

[1] Institute Pprime, CNRS UPR 3346 Poitiers University, Futuroscope, 86962 Chasseneuil, France

low-temperature/high-stress regimes. One possible explanation is the occurence of core transformations between dislocations. Another possibility is that dislocations in the two regimes are nucleated in well-separated stress and temperature conditions. A decade ago, transmission electronic microscopy experiments by Asaoka et al. revealed that in silicon perfect dislocations, nucleated at low temperature and high stress, would dissociate at a temperature ranging between 673 and 973 K [19]. These experiments were confirmed by additional investigations [20]. However, a study by Rabier and Demenet leads to the opposite conclusion that no dislocation core transformation occurs for temperatures up to 958 K [27]. Recently, Li and Picu have tried to address this issue by means of molecular dynamics simulations [28], also in silicon. They showed that no core transformation would occur by annealing only, but requires a large and well-oriented stress.

In order to shed light on this fundamental issue, I have performed atomistic calculations to determine the energy barriers associated with the transformation of a non-dissociated screw dislocation into two 30° Shockley partial dislocations, in the case of silicon. The choices of silicon and of the screw dislocation allow for a straightforward comparison with the aforementioned studies.

Numerical simulations

Atomistic simulations were performed using interatomic interactions described by the environment-dependent interatomic potential (EDIP), which has been specifically developed for modeling defects in silicon [29]. This potential is considered reliable for determining dislocation core properties [30–32]. Bulk calculations yield a lattice parameter a_0 equal to 5.4305 Å and a cohesive energy of 4.65 eV, as well as elastic constants $C_{11} = 175$ GPa, $C_{12} = 62$ GPa, and $C_{44} = 71$ GPa. Quenched molecular dynamics calculations were performed to obtain stable low-energy structures for all considered configurations. In a second stage, the nudged elastic band (NEB) technique [33] was used to determine the minimum energy paths and the activation energies between successive stable states, with 20 replicas in all cases. For an accurate calculation of the saddle state, the climbing image algorithm was employed [34]. The latter forces the image with the highest energy to climb up along the elastic band, leading to convergence toward the highest saddle point. Both relaxation and NEB computations were performed using a home-made version of the molecular dynamics code XMD [35], including implementations of the NEB method and EDIP.

The calculations were performed using a supercell oriented along the usual axis for dislocation modeling, i.e., $\hat{x} = [1\bar{2}1]$, $\hat{y} = [111]$, and $\hat{z} = [10\bar{1}]$. The supercell includes 8400 atoms, with dimensions being $20 \times 42 \times 10$ (6.651 nm 6.584 nm $\times$ 3.840 nm). A screw, a 30° partial, or a couple of 30° partial dislocations were introduced in the center of the supercell, with the dislocation line along the $\hat{z}$-axis, using displacements calculated with anisotropic elasticity theory [1] and the elastic constants calculated with EDIP. Periodic boundary conditions were applied along the $\hat{z}$-axis only, to model straight dislocations of infinite lengths. Along the $\hat{x}$- and $\hat{y}$-axis, surface boundary conditions were used, and atoms at the cell faces were kept at locations defined by the elasticity theory during simulations.

Screw and 30° partial dislocations

Thanks to numerous studies, there is a general consensus concerning the dislocations associated with the plastic deformation of silicon in the ductile regime, i.e., at temperatures greater than the BDT. In fact, plasticity occurs through the multiplication and expansion of hexagonal dislocation loops composed of 60° and screw segments, both lying along ⟨110⟩ directions and moving in the so-called "glide" set of {111} planes [1, 36]. Both dislocations are dissociated into Shockley partials, the screw into two 30° and the 60° into one 30° and one 90°, as in FCC materials. These partial dislocations bound an intrinsic stacking fault of width 6–10 nm [37, 38]. The core of these dislocations has been extensively studied [39, 40]. The 30° partial dislocation core is reconstructed along the dislocation line, with a periodicity of $\sqrt{2}a_0$ [41]. For the 90° core, two configurations have been proposed [42, 43], their core energies being so close that it is likely that both dislocations could be present at finite temperatures [44].

At low temperatures, below the BDT, there are less certainties. On one hand, it is now commonly agreed that dislocations are non-dissociated in this regime, and glide in the so-called "shuffle" set of {111} planes [26]. But on the other hand, those are found to be lying not only along ⟨110⟩ orientations, but also along unexpected ⟨112⟩ and ⟨123⟩ orientations [26, 45]. The cores of dislocations with these peculiar orientations have not been identified up to now. Nevertheless, more information is available regarding non-dissociated ⟨110⟩ dislocations. Hence, two possible stable core structures have been identified for the screw dislocation, depending on whether the dislocation core is located at the center of an hexagon (A, {111} shuffle set, Fig. 1) or at a bond center (C, {111} glide set, same figure) [26, 46]. In the latter case, the dislocation core, C_2, is reconstructed along the dislocation line with the same periodicity than the 30° partial dislocation core. The

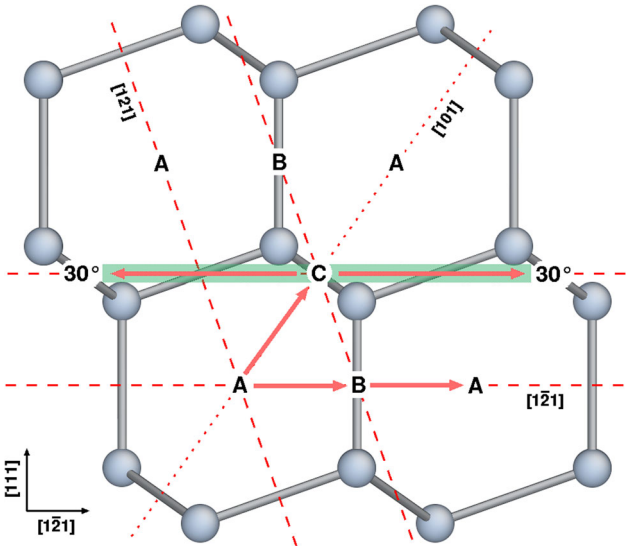

Fig. 1 Possible positions of a screw dislocation (*A*, *B*, and *C*) in the *cubic diamond* lattice, with the {111} slip planes represented by *thin dashed lines*. The *thick arrows* show the dislocation core transformation path from *A* to *C*, followed by the dissociation in two 30° partial dislocations, which borders a stacking fault (*green area*) (Color figure online)

unreconstructed structure, C_1, was found to be unstable [26]. First-principles calculations revealed that the A core is more mobile than the C_2 core [31, 47, 48], whereas the C_2 core is more stable [49, 50]. Note that another configuration corresponding to the location B is marked in Fig. 1. It has been shown to be a saddle point during screw dislocation displacement [51]. Another investigated case is the non-dissociated 60° dislocation core, which is assumed to be active for relaxing stresses in epitaxial thin films [52] or in loaded nanowires [53, 54]. It was predicted that only one core configuration could be involved in plastic deformation. However, this configuration exhibits a transient character, i.e., it becomes unstable at rest [55]. A different core structure is found to be energetically favored, albeit it was shown to be sessile in the allowed ranges of stress and temperature.

This overview of dislocations in silicon strongly suggests that it is best to investigate the dissociation of the perfect screw into two 30° partials, rather than the dissociation of the perfect 60° dislocation. This conclusion is based on several reasons listed below:

- the geometry of non-dissociated dislocation cores is better known for the screw dislocation than for the 60° dislocation;
- no 60° dislocation segments have been identified in experiments;
- the screw dislocation dissociation yields 30° partial dislocations only, for which a single core configuration is possible unlike the 90° partial;
- one intermediate step of the screw dissociation process has been revealed in a previous study [32].

In the following, I will then investigate the mechanisms leading to the dissociation of the screw dislocation. Figure 1 represents the different possible positions of a screw dislocation line in a {110} plane. Stable screw dislocation configurations correspond to C_2 and A locations. In the first case, the screw can directly dissociate into two 30° partials located in the same {111} slip plane (dashed lines in Fig. 1). In this work, I have focussed on this specific mechanism. In the second case, the A dislocation should first migrate from A to C_2, along the [101] direction (dotted line, Fig. 1). This path was investigated by Guénolé et al. using the EDIP potential [54]. They showed that the A→C_2 core transformation could occur, thanks to a thermally activated mechanism, the activation energy being 2.31 eV, with little influence of stress. The C_2 screw configuration is then a stable intermediate step during the A→C_2 → 30° + 30° transformation. Note that another possible transformation path could be A→B→ 30° + 30°. Nevertheless, such a mechanism is likely to be more complicated than the one previously depicted, with a higher activation energy. In fact, a screw dislocation in B position is not stable and then could not be an intermediate step.

It is instructive to compare the core geometries of the 30° partial dislocation (see for instance Figs. 2a or 3b) with the C_2 screw dislocation (Figs. 3a or 4a). They are both characterized by the presence of dimers oriented along $[10\bar{1}]$ due to the reconstruction, leading to a similar core periodicity of $\sqrt{2}a_0$ along this orientation. The main difference is the presence of two lines of such dimers for the C_2 screw dislocation, arranged in a staggered pattern, while there is only one for the 30° partial dislocation. Then the C_2 dislocation core can be considered as the direct geometrical juxtaposition of two reconstructed 30° dislocations (with a $a_0/\sqrt{2}$ shift along $[10\bar{1}]$). Note that relaxing an initial configuration including two adjacent unreconstructed 30° dislocations yields a C_1 dislocation core instead.

Because of this similarity of core geometry, it is reasonable to expect that the mechanisms leading to the displacement of the 30° partial dislocation could be involved in the dissociation process as well. Then I have first investigated the migration of a single 30° partial dislocation with the simulation setup previously described. It is commonly agreed that dislocation displacement is associated with the formation of kink pairs followed by kinks' migration along the dislocation line [1]. Unfortunately, the issue lies in the complexity of possible kink configurations, especially when they are combined with reconstruction defects (see for instance [58] for a discussion about this point). Here, I have considered the four kink configurations

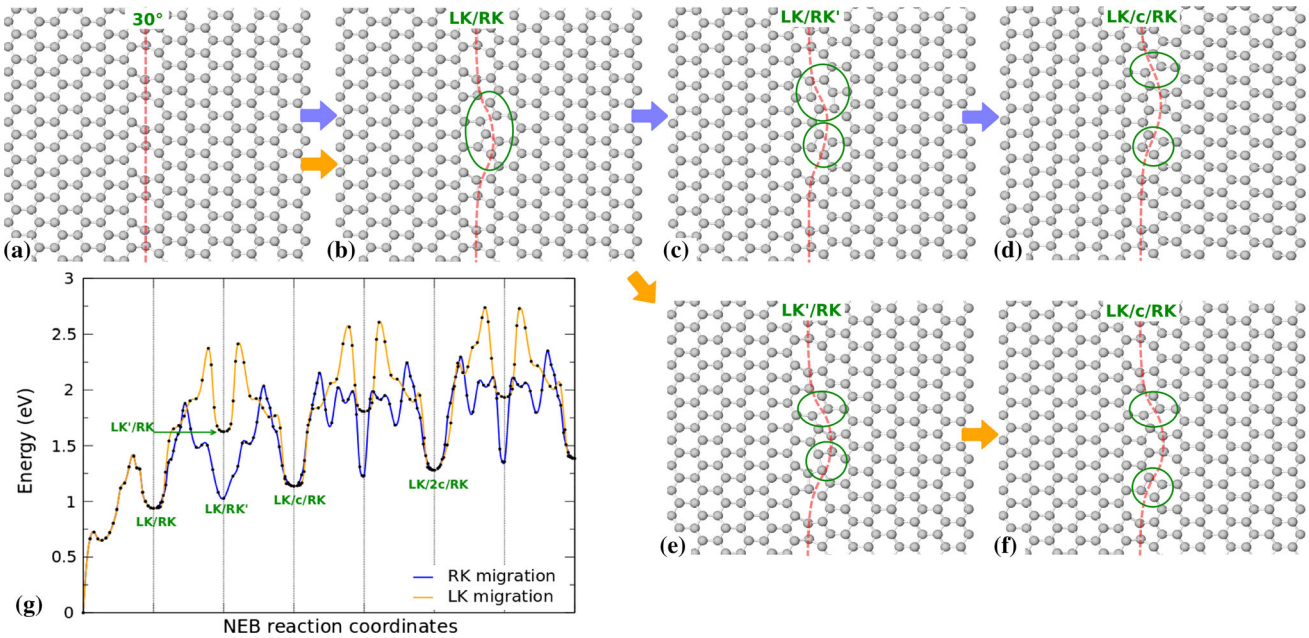

Fig. 2 **a–f** Atomistic configurations (slice along [111]) and **g** NEB calculated energies for kinks pair formation and migration in the case of a 30° partial dislocation. After the initial formation (**a**, **b**) of a pair of kinks (*left*, LK, and *right*, RK), the dislocation displacement occurs through the migration of RK (**b–d**, *blue curve* in *g*) or LK (**b–e–f**, *orange curve* in *g*). LK′ and RK′ are intermediate configurations along the migration paths of LK and RK, respectively. *c* is the length of one translation unit along the reconstructed 30° partial dislocation core and is equal to $\sqrt{2}a_0$ (Color figure online)

usually reported in the literature [57], with the aim of (i) validating our setup and (ii) having elements of comparison for the C_2 screw dissociation.

Figure 2 shows the first steps of the 30° partial dislocation displacement, initiated by the formation of a pair of LK and RK kinks (Fig. 2b), and followed by the migration of either the RK kink (Fig. 2b–d) or the LK kink (Fig. 2b, e, f). The associated energy variations, calculated with the NEB technique, are reported in Fig. 2g. In agreement with previous investigations, RK′ and LK′ are intermediate configurations during the RK and LK kink migration, respectively. They are found to be energetically less stable than RK and LK, respectively. The structures of LK, LK′, RK, and RK′ kinks are in excellent agreement with those reported in the literature [57]. Note however that the NEB calculated energy variations in Fig. 2g appear to be more complex than those in earlier works (see for instance [56]), and include several minor inflection points or weakly stable minima. This is probably due to the large number of images in the present NEB calculations, and some might be non-physical. In fact, interatomic potentials based on complex mathematical expressions are more prone to yield such inflections in energy variations [60]. Nevertheless, the overall shape of the migration energy paths is in good agreement with previous works, and the most important point along the path, the one with the highest energy, does not depend on these inflections and minima.

The calculated barrier for the first step of the RK + LK kink pair formation is 1.41 eV. An alternative computed path leads to the formation of a stable RK′ + LK′ kink pair, with a greater activation energy of 2.33 eV. Increasing the separation between kinks, the energy variations tend to converge to a shape characteristic of a single kink migration. In Table 1, several formation and migration energies are reported, obtained by extrapolating the NEB results to large kink separations, and compared to earlier investigations. These energies are overall in good agreement with previous calculations, although it is difficult to understand why the kink formation values are closer to those obtained with the SW potential [56] or tight binding [57], than those obtained with EDIP in an earlier work [30].

C_2 screw dissociation

I now focus on the dissociation mechanism of the C_2 screw dislocation into two 30° partial dislocations. First, the energy difference between these two systems, with an increasing separation d between the partial dislocations, is calculated. The result is shown in Fig. 3, along with the corresponding atomistic configurations. d is computed as the average $\hat{x}$-position difference of the central core atoms of the 30° partial dislocations. d increases with steps of $\sqrt{6}a_0/4$, except for the initial step being approximately

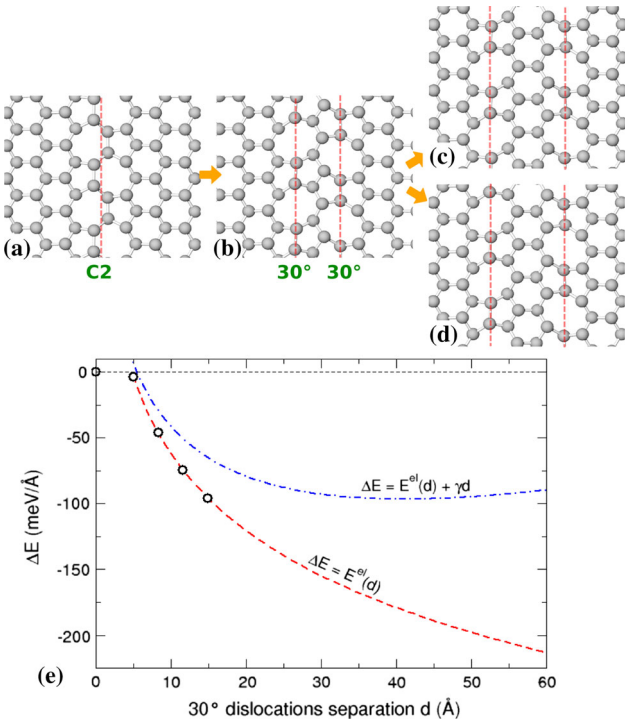

Fig. 3 **a–d** Stable configurations, from a whole C_2 screw dislocation (**a**) to two 30° partial dislocations with an increasing separation (**b–d**). **e** Energy difference, relative to the C_2 screw dislocation, as a function of the separation d. The red curve is a fit using the calculated energies (*filled circles*) and the expression 1. The *blue curve* shows the effect of adding the stacking fault energy contribution, missing in EDIP calculations, with a value $\gamma = 33$ mJ/m^2 [59] (Color figure online)

$3\sqrt{6}a_0/8$. It appears that there is an energy gain even for the shortest separation. This is in agreement with a similar calculation performed in diamond, albeit with a different screw core configuration [61]. In Fig. 3, one can see that there are two different configurations for $d = 5\sqrt{6}a_0/8$ (and larger separations with the period $\sqrt{6}a_0/2$). In one case, the dimer lines in the two 30° cores are aligned along $[10\bar{1}]$ (Fig. 3c), whereas they are shifted by $a_0/\sqrt{2}$ along the same direction (Fig. 3d). A negligible energy difference between these two configurations was calculated in all cases.

According to elasticity theory and assuming isotropy, the energy variation for larger separations should follow the interaction energy between two dislocations [1], i.e.,

$$E^{el} = -\frac{\mu}{2\pi}\left[(\mathbf{b_1}\cdot\xi)(\mathbf{b_2}\cdot\xi) + \frac{(\mathbf{b_1}\times\xi)(\mathbf{b_2}\times\xi)}{1-\nu}\right]\ln\left(\frac{d}{r_0}\right). \quad (1)$$

Consequently, the calculated energy variations for $d \neq 0$ is fitted with the expression $\Delta E = E^{el} = \alpha \ln d/\beta$, the two parameters α and β being the elastic factor and the core radius, respectively. The best fit is obtained with $\alpha = 84$ meV/Å and $\beta = 4.81$ Å (Fig. 3). Note that the dissociation of the screw dislocation is accompanied by the creation of an intrinsic stacking fault bordered by the 30° partial dislocations. The energy penalty associated with the stacking fault expansion leads to a restoring force, which opposes to the repulsive interaction between partial dislocations. This effect is not present in our calculations since the stacking fault energy is zero when calculated with EDIP, as it is often the case with short-ranged bond order interatomic potentials. A corrected energy variation is represented in Fig. 3, simply obtained by adding γd (blue curve), with $\gamma = 33$ mJ/m^2 determined using first-principles calculations [59]. With this correction, the dissociation width is predicted to be 4 nm in good agreement with experiments.

As expected, the previous calculation indicates that the screw dislocation dissociation is energetically favored, even for the shortest separation. But the energy barriers associated to the lattice friction hindering the motion of the 30° partial dislocations are missing. NEB calculations have then been performed to determine the minimum energy paths associated with the formation and migration of kinks leading to the first dissociation steps. Considering the structural similarities between C_2 and 30° cores, configurations including stable kinks similar to those obtained for the 30° dislocation displacement have been used as endpoints in NEB calculations. The final minimum energy paths and the associated energy variations are represented in Fig. 4. The computed mechanisms lead to the dissociation of the C_2 screw dislocation by the formation of an LK + RK kink pair first, followed by the migration of one or the other kink along the dislocation line.

Starting with the initial step, it is found that the stable kink pair LK + RK is structurally close to the LK + RK kink pair obtained in the case of a single 30° partial dislocation (Figs. 2b, 4b). But its formation energy is lower (0.52 eV compared to 0.94 eV). The formation path is similar for both cases. Nevertheless, the corresponding energy barrier is 2.14 eV for the C_2 dissociation, i.e., substantially higher than the value of 1.41 eV for the single 30° partial dislocation. I also considered the formation of an LK′ + RK′ pair as a first dissociation step. In that case, the computed formation energy of 1.42 eV is much larger than that for the LK + RK pair, although the associated energy barrier of 2.37 eV is comparable. The computed migration mechanisms of LK and RK (Fig. 4b–f) are also similar to those obtained in the case of the single 30° partial dislocation. Both LK′ and RK′ are stable intermediate configurations along the LK and RK displacement, and migration energies are about 1.4 and 1.3 eV, respectively. The LK value is the same as for the single 30° partial dislocation, while the RK value is slightly higher.

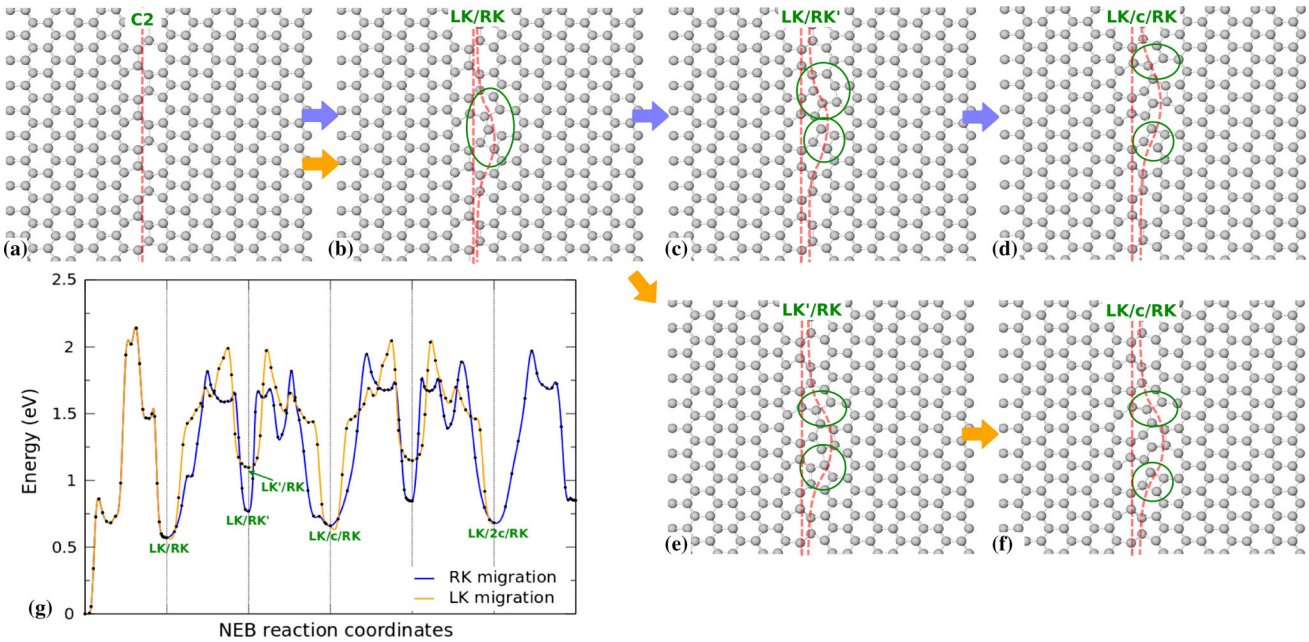

Fig. 4 **a–f** Atomistic configurations (slice along [111]) and (**g**) NEB calculated energies for kink pair formation and migration associated to the first dissociation steps of a C_2 screw dislocation. After the initial formation (**a**, **b**) of a pair of kinks (*left*, LK, and *right*, RK), the dislocation displacement occurs through the migration of RK (**b–d**, *blue curve* in **g**) or LK (**b–e–f**, *orange curve* in **g**). LK′ and RK′ are intermediate configurations along the migration paths of LK and RK, respectively. *c* is the length of one translation unit along the reconstructed C_2 screw dislocation core, and is equal to $\sqrt{2}a_0$ (Color figure online)

Table 1 Kink formation (F_k) and migration (W_m) energies (in eV), computed in this work (first column) and from earlier numerical simulations using the same potential (EDIP [30]), the Stillinger–Weber (SW) potential [56], and tight binding [57].

	EDIP	EDIP [30]	SW [56]	TB [57]
F_k(LK + RK)	1.6	1.37	1.63	1.57
F_k(LK′ + RK′)	2.2	1.88	2.13	2.61
W_m(LK→LK′)	1.4	1.46	0.82	1.52
W_m(LK′→LK)	0.8	0.84	0.4	1.09
W_m(RK→RK′)	1.0	1.22	0.74	2.03
W_m(RK′→RK)	1.0	0.89	0.82	1.62

Overall, it is observed that the first steps leading to the dissociation of the C_2 dislocation are comparable to those leading to the displacement of a single 30° partial dislocation. I already mentioned that it is not surprising given the related structures of the two initial configurations. According to this result, only the first dissociation steps were investigated, for one should quickly recover the behavior of a single 30° partial dislocation for larger separations *d*. The most important conclusion here is that it is the formation of the initial stable LK + RK kink pair which requires the highest energy activation during the C_2 screw dissociation. This first step is then the limiting process, with an activation energy of 2.14 eV.

Summary

The calculations reported here have lead to the following conclusions:

- the dissociation of a C_2 screw dislocation into two 30° partial dislocations occurs by the formation of kink pairs, followed by the migration of one or the other kink along the dislocation line;
- these kinks are structurally very close to kinks associated with the displacement of a single 30° partial dislocation, even for the first dissociation step;
- the activation energy for the whole dissociation mechanism is 2.14 eV.

The second point above can be explained by the strong similarity between the C_2 screw and 30° partial cores. Nevertheless, one may argue that these kinks are obtained mainly because they were initially introduced as stable mid-points for NEB calculations. Additional calculations have then been performed for determining other stable configurations, in particular for the first dissociation step. Those yield alternative solutions, but a structural analysis revealed that they are combination of kinks and core reconstruction defects (LC and RC, following the notations in [57]) and that large energy barriers have to be overcome for their formation. Therefore, it is reasonable to conclude that the mechanism described in the previous sections is most likely to dissociate the screw dislocation.

Considering now the activation energy of 2.14 eV, it is interesting to notice that it is slightly lower than the activation energy associated with the screw dislocation core transformation $A \rightarrow C_2$ (2.3 eV [32], calculated with the same potential). Then, if this core transformation is thermally activated, the screw dissociation should also take place. The activation energies in the range of 2.1–2.3 eV are relatively large, suggesting that temperatures as high as about 900 K are required for these processes to occur in an experiment. Godet et al. have shown that at these temperatures there is a change in the nature of nucleated dislocations [62]. It is then difficult to discriminate between dissociation and nucleation, and both could be responsible for the observed transition in experiments [19, 20, 27].

The dissociation of dislocations in annealing experiments has been observed at 600 K [21]. The activation energies calculated in this work then appear slightly too high. One possible cause is the overestimation of these energies using EDIP. The effect of stress also has not been considered here and might help lower the reported activation energies. In fact, a recent molecular dynamics study by Li and Picu revealed that screw dislocation dissociation could be favored in the presence of a specific stress state [28]. This might explain contradicting experimental results, as well as the existence of two transition temperatures [21].

Acknowledgements I am indebted to Prof. Sandrine Brochard and Dr. Jacques Rabier for our discussions and their comments on this work.

Compliance with ethical standards

Conflict of Interest The author declares that he has no conflict of interest.

References

1. Hirth JP, Lothe J (1982) Theory of dislocations. Wiley, New York
2. Masolin A, Bouchard PO, Martini R, Bernacki M (2013) Thermo-mechanical and fracture properties in single-crystal silicon. J. Mater. Sci. 48:979. doi:10.1007/s10853-012-6713-7
3. Han X, Zheng K, Zhang Y, Zhang X, Zhang Z, Wang ZL (2007) Low-temperature in situ large-strain plasticity of silicon nanowires. Adv. Mater. 19(16):2112
4. Gordon M, Baron T, Dhalluin F, Gentile P, Ferret P (2009) Size effects in mechanical deformation and fracture of cantilevered silicon nanowires. Nanoletters 9(2):525
5. Tang DM, Ren CL, Wang MS, Wei X, Kawamoto N, Liu C, Bando Y, Mitome M, Fukata N, Golberg D (2012) Mechanical properties of si nanowires as revealed by in sit transmission electron microscopy and molecular dynamics simulations. Nanoletters 12:1898
6. Kang W, Saif MTA (2013) In situ study of size and temperature dependent brittle-to-ductile transition in single crystal silicon. Adv Funct Mater 23(6):713–719
7. Lieber C (2011) Semiconductor nanowires: a platform for nanoscience and nanotechnology. Mater Res Soc Bull 36:1052
8. Shao R, Zheng K, Zhang Y, Li Y, Zhang Z, Han X (2012) Piezoresistance behaviors of ultra-strained sic nanowires. Appl Phys Lett 101(23):233109
9. Michler J, Wasmer K, Meier S, Östlund F, Leifer K (2007) Plastic deformation of gallium arsenide micropillars under uniaxial compression at room temperature. Appl Phys Lett 90(4):3123
10. Östlund F, Rzepiejewska-Malyska K, Leifer K, Hale LM, Tang Y, Ballarini R, Gerberich WW, Michler J (2009) Nanostructure fracturing: brittle-to-ductile transition in uniaxial compression of silicon pillars at room temperature. Adv. Funct. Mater. 19(15): 2439–2444
11. Korte S, Barnard J, Stearn R, Clegg W (2011) Deformation of silicon—insights from microcompression testing at 25–500 °c. Int J Plast 27:1853
12. Thilly L, Ghisleni R, Swistak C, Michler J (2012) In situ deformation of micro-objects as a tool to uncover the micro-mechanisms of the brittle-to-ductile transition in semiconductors: the case of indium antimonide. Philos. Mag. 92(25–27):3315–3325
13. Shin C, Jin HH, Kim WJ, Park JY (2012) Mechanical properties and deformation of cubic silicon carbide micropillars in compression at room temperature. J Am Chem Soc 95(9):2944
14. Deneen J, Mook W, Minor A, Gerberich W, Barry Carter C (2006) In situ deformation of silicon nanospheres. J Mater Sci 41(14):4477–4483. doi:10.1007/s10853-006-0085-9
15. Gerberich WW, Stauffer DD, Beaber AR, Tymiak NI (2012) A brittleness transition in silicon due to scale. J Mater Res 27:552–561
16. Ishida T, Cleri F, Kakushima K, Mita M, Sato T, Miyata M, Itamura N, Endo J, Toshiyoshi H, Sasaki N, Collard D, Fujita H (2011) Exceptional plasticity of silicon nanobridges. Nanotechnology 22(35):355–704
17. Rabier J, Montagne A, Demenet JL, Michler J, Ghisleni R (2013) Silicon micropillars: high stress plasticity. Phys Stat Sol (c) 10(1):11
18. Izumi S, Ohta H, Takahashi C, Suzuki T, Saka H (2010) Shuffle-set dislocation nucleation in semiconductor silicon device. Philos Mag Lett 90(10):707
19. Asaoka K, Umeda T, Arai S, Saka H (2005) Direct evidence for shuffle dislocations in si activated by indentations at 77k. Mater Sci Eng A 400–401:93
20. Saka H, Yamamoto K, Arai S, Kuroda K (2006) In-situ tem observation of transformation of dislocations from shuffle to glide sets in si under supersaturation of interstitials. Philos Mag 86(29–31):4841
21. Okuno T, Saka H (2013) Electron microscope study of dislocations introduced by deformation in a si between 77 and 873k. J Mater Sci 48:115. doi:10.1007/s10853-012-6860-x
22. Suzuki T, Nishisako T, Taru T, Yasutomi T (1998) Plastic deformation of InP at temperatures between 77 and 500k. Philos Mag Lett. 77(4):173
23. Suzuki T, Yasutomi T, Tokuoka T, Yonenaga I (1999) Plastic deformation of GaAs at low temperatures. Philos Mag A 79(11):2637
24. Rabier J, Cordier P, Demenet JL, Garem H (2001) Plastic deformation of si at low temperature under high confining pressure. Mater Sci Eng A 309–310:74
25. Kedjar B, Thilly L, Demenet JL, Rabier J (2010) Plasticity of indium antimonide between -176 and 400 c under hydrostatic pressure. Part i: macroscopic aspects of the deformation. Acta Mater 58:1418
26. Rabier J, Pizzagalli L, Demenet JL (2010) Dislocations in silicon at high stress (chap. 93). In: Kubin L, Hirth JP (eds) Dislocation in solids, vol 16. Elsevier, New York, p 47
27. Rabier J, Demenet JL (2005) On the nucleation of shuffle dislocations in si. Phys Stat Sol (a) 5(5):944

28. Li Z, Picu R (2013) Shuffle-glide dislocation transformation in si. J Appl Phys 113:83–519
29. Justo JF, Bazant MZ, Kaxiras E, Bulatov VV, Yip S (1998) Interatomic potential for silicon defects and disordered phases. Phys Rev B 58(5):2539
30. Justo JF, Bulatov VV, Yip S (1999) Dislocation core reconstruction and its effect on dislocation mobility in silicon. J Appl Phys 86(8):4249–4257
31. Pizzagalli L, Pedersen A, Arnaldsson A, Jónsson H, Beauchamp P (2008) Theoretical study of kinks on screw dislocation in silicon. Phys Rev B 77:064–106
32. Guénolé J, Godet J, Pizzagalli L (2010) Determination of activation parameters for the core transformation of the screw dislocation in silicon. Model Simul Mater Sci Eng 18:065001
33. Jónsson H, Mills G, Jacobsen KW (1998) Nudged elastic band method for finding minimum energy paths of transitions (chap. 16). In: Berne BJ, Ciccotti G, Coker DF (eds) Classical and quantum dynamics in condensed phase simulations. World Scientific, Singapore, p 385
34. Henkelman G, Uberuaga BP, Jónsson H (2000) A climbing image nudged elastic band method for finding saddle points and minimum energy paths. J Chem Phys 113(22):9901
35. Rifkin J http://xmd.sourceforge.net/
36. Kubin L (2013) Dislocations, mesoscale simulations and plastic flow. Oxford series on materials modelling. Oxford University Press, London
37. Ray I, Cockayne D (1971) The dissociation of dislocations in silicon. Proc R Soc Lond A 325:543
38. Wessel K, Alexander H (1977) On the mobility of partial dislocations in silicon. Philos Mag 35:1523
39. Kolar HR, Spence JCH, Alexander H (1996) Observation of moving dislocation kinks and unpinning. Phys Rev Lett 77(19):4031
40. Lehto N, Heggie MI (1999) Modelling of dislocations in c-si. In: Hull R (ed), Properties of crystalline silicon, no. 20 in EMIS Datareviews, p 357. INSPEC, London (1999)
41. Duesbery MS, Joos B, Michel DJ (1991) Dislocation core studies in empirical silicon models. Phys Rev B 43(6):5143
42. Bigger JRK, McInnes DA, Sutton AP, Payne MC, Stich I, King-Smith RD, Bird DM, Clarke LJ (1992) Atomic and electronic structures of the 90° partial dislocation in silicon. Phys Rev Lett 69(15):2224
43. Bennetto J, Nunes RW, Vanderbilt D (1997) Period-doubled structure for the 90° partial dislocation in silicon. Phys Rev Lett 79(2):245
44. Lehto N, Öberg S (1998) Effects of dislocation interactions: application to the period-doubled core of the 90° partial in silicon. Phys Rev Lett 80(25):5568
45. Rabier J, Cordier P, Tondellier T, Demenet JL, Garem H (2000) Dislocation microstructures in si plastically deformed at rt. J Phys Condens Matter 12(49):10–59
46. Pizzagalli L, Godet J, Guénolé J, Brochard S (2012) Dislocation cores in silicon: new aspects from numerical simulations. J Phys Conf Ser 281:012002
47. Pizzagalli L, Beauchamp P (2004) First principles determination of the Peierls stress of the shuffle screw dislocation in silicon. Philos Mag Lett 84(11):729
48. Pizzagalli L, Beauchamp P (2008) Dislocation motion in silicon: the shuffle-glide controversy revisited. Philos Mag Lett 88(6):421
49. Pizzagalli L, Beauchamp P, Rabier J (2003) Undissociated screw dislocations in silicon: calculations of core structure and energy. Philos Mag A 83:1191
50. Wang CZ, Li J, Ho KM, Yip S (2006) Undissociated screw dislocation in si: glide or shuffle set? Appl Phys Lett 89:051–910
51. Pizzagalli L, Beauchamp P, Jónsson H (2008) Calculations of dislocation mobility using nudged elastic band method and first principles DFT calculations. Philos Mag 88(1):91
52. Marzegalli A, Montalenti F, Miglio L (2005) Stability of shuffle and glide dislocation segments with increasing misfit in ge/si_{1-x}(001) epitaxial layers. Appl Phys Lett 86:041–912
53. Kang K, Cai W (2007) Brittle and ductile fracture of semiconductor nanowires—molecular dynamics simulations. Philos Mag 87(14–15):2169
54. Guénolé J, Godet J, Brochard S (2011) Deformation of silicon nanowires studied by molecular dynamics simulations. Model Simul Mater Sci Eng 19(7):074003
55. Pizzagalli L, Godet J, Brochard S (2009) Glissile dislocations with transient cores in silicon. Phys Rev Lett 103:065–505
56. Bulatov VV, Yip S, Argon AS (1995) Atomic modes of dislocation mobility in silicon. Philos Mag A 72(2):453
57. Nunes RW, Bennetto J, Vanderbilt D (1998) Core reconstruction of the 90° partial dislocation in nonpolar semiconductors. Phys Rev B 58(19):12563
58. Bulatov VV, Justo JF, Cai W, Yip S, Argon AS, Lenosky T, de Koning M, de la Rubia TD (2001) Parameter-free modelling of dislocation motion: the case of silicon. Philos Mag A 81(5):1257
59. Chou MY, Cohen ML, Louie SG (1985) Theoretical study of stacking faults in silicon. Phys Rev B 32:7979–7987
60. Godet J, Pizzagalli L, Brochard S, Beauchamp P (2003) Comparison between classical potentials and ab initio methods for silicon under large shear. J Phys: Condens Matter 15:6943
61. Blumenau AT, Jones R, Frauenheim T, Willems B, Lebedev OI, Tendeloo GV, Fisher D, Martineau PM (2003) Dislocations in diamond: dissociation into partials and their glide motion. Phys Rev B 68:14115
62. Godet J, Hirel P, Brochard S, Pizzagalli L (2009) Evidence of two plastic regimes controlled by dislocation nucleation in silicon nanostructures. J Appl Phys 105:026–104